Supplemental Information

Escherichia coli NusG Links the Lead Ribosome

with the Transcription Elongation Complex

Robert S. Washburn, Philipp K. Zuber, Ming Sun, Yaser Hashem, Bingxin Shen, Wen Li, Sho Harvey, Francisco J. Acosta Reyes, Max E. Gottesman, Stefan H. Knauer, and Joachim Frank

Supplemental Tables

Table S1: Electron Microscopy and Modeling. Related to Figure 1.

Data collection	Polara-F30
Micrographs	1,327
Picked Particles	188,127
Voltage (KV)	300
Pixel size (Å/pixel)	1.66
Structure	
Component	70S:NusG
Particles	17,122
FSC 0.143 (Å)	6.8
Model Refinement	
Component	30S:NusG
Program/Protocol	MDFF/Phenix
Used in refinement (Å)	6.8
Average B-factors ($Å^2$)	556.01
Avg B-fac Prot/RNA ($Å^2$)	571.78/546.93
R.m.s deviations:	
Bonds (Å)	0.009
Angles (deg)	1.123
Validation	
Molprobity score	1.61
Clashcore, all atoms	2.59
Rotamer outliers (%)	1.85
Ramachandran plot:	
Outliers (%)	0.17
Allowed (%)	5.15
Favored (%)	94.68
Composition	
Non hydrogen atoms	52,035
Protein residues	2,413
RNA bases	1,539
Ligands	0
Accession codes	
EMDB	EMD-22143
PDB	6XE0

Supplemental Figures
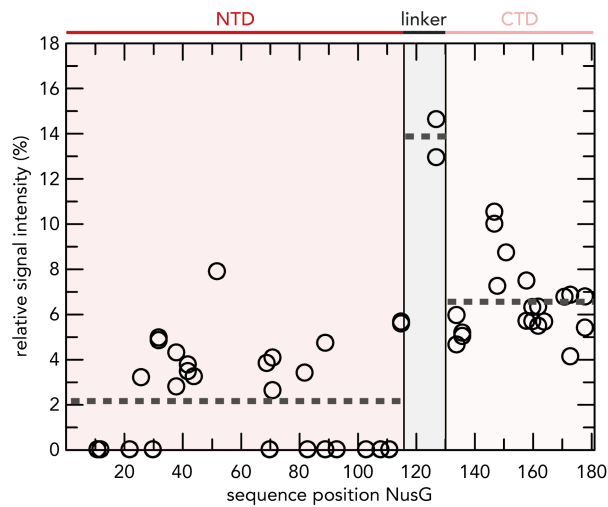
Figure S1: Binding of [ILV]-NusG to RNAP. Related to Figure 2B. $[^{1}H,^{13}C]$-methyl-TROSY derived relative signal intensities of [ILV]-NusG methyl groups after addition of two equivalents of RNAP (see Fig. 2B). Dashed horizontal lines indicate average relative signal intensities of NusG-NTD, the linker, and NusG-CTD (domain organization is indicated at the top).
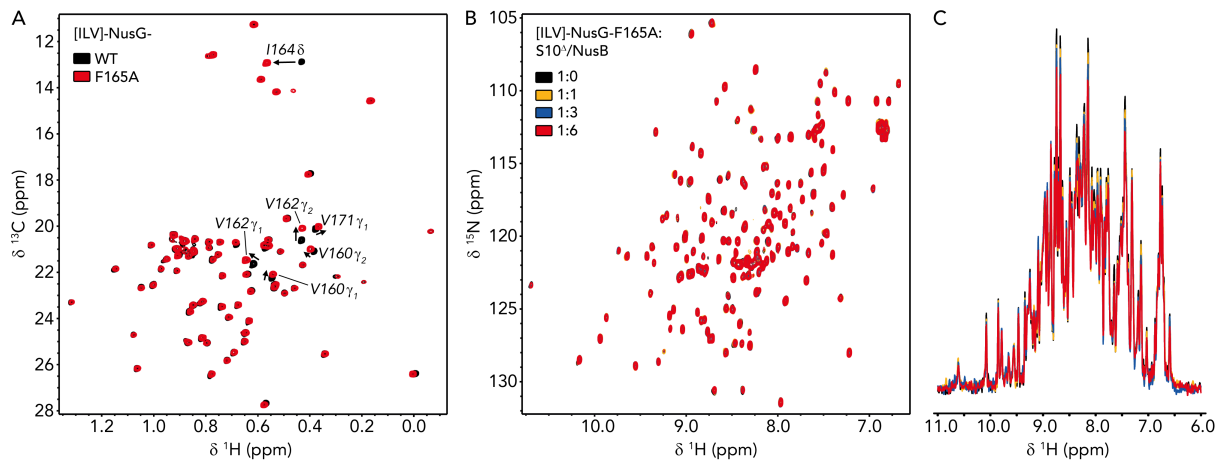
Figure S2: NusG^{F165A} does not interact with S10$_Δ$:NusB. Related to Figure 3. **(A)** 2D [^{1}H, ^{13}C]-methyl-TROSY spectra of [ILV]-NusG (11 μM, black) and [ILV]-NusG^{F165A} (20 μM, red). Arrows and labels indicate NusG-CTD methyl groups affected in their resonance frequencies by the F165A amino acid substitution. **(B,C)** 2D **(B)** and normalized 1D **(C)** [^{1}H, ^{15}N]-HSQC spectra of 20 μM [ILV]-NusG^{F165A} upon titration with 432 μM S10$_Δ$:NusB (colors as indicated).

Transparent Methods

Strain construction. Standard bacteriological techniques used in strain construction (e.g., transformation, transduction and media preparation) are as described in (Silhavy et al., 1984). Standard molecular biology techniques were as described in Sambrook and Russell (Sambrook and Russel, 2001). N10780 was constructed by P1 transduction of *rpoC-his:kanR nusGF165A* from NB885 into MDS42. N11158 was constructed by P1 transduction of *ΔssrA::camR* from RSW943 into MDS42. N11816 was constructed by P1 transduction of *ΔrelA::kanR* from RLG847 into N11158. RSW1008 was constructed by P1 transduction of *ΔssrA::camR* from RSW943 into N4837. RSW1010 was constructed by P1 transduction of *rpoC-his:kanR nusGF165A* from NB885 into N4837. RSW1012 was constructed by P1 transduction of *ΔssrA::camR* from RSW943 into RSW1010. RSW1175 was constructed by P1 transduction of *ΔrelA::kanR* and *ΔspoT::camR* from RLG847 into MDS42. RSW1245 was generated using recombineering (Sharan et al., 2009) to introduce six rare arginine codons (atg-acc-atg-AGG-AGA-CGA-AGG-AGA-CGA-att-acg-gat) into the 5'end of *lacZ* in MDS42 changing the amino acid sequence of the aminoterminus from MTMITD to MTMRRRRRRITD with six inefficiently translated arginine codons. RSW1225 was produced using recombineering to introduce two G to A mutations in the ribosome binding site of *lacZ* in MDS42. This resulted in a change from …TTCACACAGGAAACAGCTatgaccatg… to …TTCACACACC AAACAGCTatgaccatg… inactivating the ribosome binding site. RSW1225 is *lac⁻*.

Cloning. The plasmid encoding NusG^F165A (pET11a_*nusG-F165A*) was generated by site-directed mutagenesis according to the QuikChange Site-Directed Mutagenesis Kit protocol (Stratagene), using vector pET11a_*nusG* (Burmann et al., 2011) as template and primers Fw_NusG-F165A (5' GTG TCT GTT TCT ATC GCG GGT CGT GCG ACC CCG 3') and

Rv_NusG-F165A (5' CGG GGT CGC ACG ACC CGC GAT AGA AAC AGA CAC 3'; both primers were obtained from metabion, Martinsried, Germany).

Protein production and isotopic labeling. For the production of unlabeled proteins, bacteria were grown in lysogeny broth (LB) medium. [^{1}H,^{13}C]-labeling of methyl groups of Ile, Leu, and Val residues in perdeuterated proteins was accomplished by growing bacteria in minimal medium M9 (Meyer and Schlegel, 1983; Sambrook and Russel, 2001) prepared with increasing amounts of D$_2$O (0 % (v/v), 50 % (v/v), 100 % (v/v); Eurisotop, Saint-Aubin, France) and (^{15}NH$_4$)$_2$SO$_4$ (CortecNet, Voisins-Le-Bretonneux, France) and d$_7$-glucose (Cambridge Isotope Laboratories, Inc., Tewksburgy, USA) as sole nitrogen and carbon sources, respectively. Amino acid precursors (60 mg/l 2-keto-3-d$_3$-4-^{13}C-butyrate and 100 mg/l 2-keto-3-methyl-d$_3$-3-d$_1$-4-^{13}C-butyrate; Eurisotop, Saint-Aubin, France) were added 1 h prior to induction. Expression and purification protocols were identical to those of non-labeled proteins.

Production of full-length NusG and NusG^{F165A} for NMR studies was based on (Burmann et al., 2011). For expression, *E. coli* BL21 (λ DE3) cells (Novagen, Madison, WI, USA) harboring plasmids pET11a_*nusG* or pET11a_*nusG-F165A* (encoding tag-less *E. coli* NusG or NusG^{F165A}, respectively) were grown in medium containing ampicillin (100 µg/ml) to an optical density at 600 nm (*OD$_{600}$*) of 0.8 at 37 °C. Overexpression was subsequently induced by addition of 1 mM isopropyl-1-thio-β-D-galactopyranoside (IPTG) and continued for 4 h at 37 °C. Cells were harvested by centrifugation (6,000 x *g*), resuspended in buffer A^{NusG} (50 mM tris(hydroxymethyl)aminomethane (Tris)/HCl (pH 7.5), 250 mM NaCl) supplemented with ½ protease inhibitor cocktail tablet (cOmplete, EDTA-free, Roche Diagnostics, Mannheim, Germany) and a small amount of DNase I (AppliChem GmbH, Darmstadt, Germany), and lysed using a microfluidizer. After clearing the lysate by centrifugation (13,000 x *g*, 30 min, 4 °C), streptomycin sulfate was added to a final

concentration of 1 % (w/v) and the solution was stirred for 30 min at room temperature to precipitate nucleic acids. Following centrifugation, the supernatant was successively supplemented with $(NH_4)_2SO_4$ at 4 °C under continuous stirring to a final concentration of 60 % (w/v). The pellet was collected by centrifugation, dissolved in buffer B^{NusG} (10 mM Tris/HCl (pH 7.5)) and subsequently dialyzed against the same buffer overnight. The solution was then applied to a 5 ml HeparinFF column (GE Healthcare, Munich, Germany) equilibrated with buffer B^{NusG}. After washing with 20 column volumes (CVs) buffer B^{NusG}, proteins were eluted using a step gradient from 50 mM – 1 M NaCl in buffer B^{NusG}. Target protein containing fractions were combined, concentrated by ultrafiltration (molecular weight cut-off (MWCO): 5 kDa), and then applied to a HiLoad S75 size exclusion chromatography (SEC) column (GE Healthcare, Munich, Germany) equilibrated with buffer C^{NusG} (4-(2-hydroxyethyl)-1-piperazineethanesulfonic acid (HEPES; pH 7.5), 100 mM NaCl). Fractions containing pure NusG/NusG^{F165A} were combined, concentrated by ultrafiltration (MWCO: 5 kDa), flash-frozen in liquid nitrogen and stored at -80 °C.

NusG for cryoEM was produced based on (Saxena et al., 2018). In brief, *E. coli* BL21 (λ DE3) cells (Novagen, Madison, WI, USA) harboring plasmid pRM431, which codes for NusG fused to a hexahistidine tag at its C-terminus, were grown in LB medium containing 100 µg/ml ampicillin at 37 °C. Upon reaching an OD_{600} of 0.5 *nusG-his$_6$* expression was induced by IPTG addition (0.5 mM) and cells were harvested 3 hours later by centrifugation (4,347 x *g*, 15 min, 4 °C). The cell pellet was resuspended in buffer D^{NusG} (50 mM Tris/HCl (pH 7.5), 150 mM NH$_4$Cl), ½ a tablet protease inhibitor (EDTA-free, Sigma-Aldrich) was added, and cells were disrupted by four freeze-thaw cycles in a dry-ice ethanol bath and water at room temperature followed by sonication (4 x 15 s pulses). The lysate was centrifuged (12,000 x *g*, 30 min, 4 °C) and the crude extract was added to Ni-NTA resin (GE Healthcare) equilibrated with buffer D^{NusG} (5 ml resin / 10 ml crude extract). After overnight incubation with rotation at 4 ° C the resin was packed in 2 ml columns and each column was washed

with 5 CVs buffer D^{NusG}. Elution was carried out with increasing imidazole concentration (100-500 mM imidazole in buffer D^{NusG}). Target protein containing fractions were combined, dialyzed against buffer E^{NusG} (20 mM Tris/HCl (pH 7.5), 100 mM NH_4Cl, 10 mM $MgCl_2$, 0.5 mM EDTA, 1 mM tris(2-carboxyethyl)phosphine (TCEP)) overnight at 4 °C, before being subjected to a SEC run using a Superdex 200 column (GE Life Sciences). Fractions containing pure His_6-NusG were combined and stored at -80 °C.

NusG-NTD was produced as was full-length NusG for NMR studies, except that plasmid pET11a_*EcNusG-NTD(1-124)*, which encodes tag-less *E. coli* NusG-NTD (residues 1-124; (Burmann et al., 2011)), was used.

NusG-CTD was produced according to (Burmann, 2010) using *E. coli* BL21 (λ DE3) cells (Novagen, Madison, WI, USA) containing plasmid pETGB1a_*nusG-CTD(123-181)* (encoding *E. coli* NusG-CTD fused to a His_6-Gb1 tag followed by a tobacco etch virus (TEV) cleavage site at its N-terminus). In brief, the conditions for expression were the same as for full-length NusG. Cells were collected by centrifugation (6,000 x *g*, 10 min, 4 °C), resuspended in buffer $A^{NusG-CTD}$ (50 mM Tris/HCl (pH 7.5), 150 mM NaCl) containing 10 mM imidazole, supplemented with ½ protease inhibitor cocktail tablet (cOmplete, EDTA-free, Roche Diagnostics, Mannheim, Germany) and a small amount of DNase I (AppliChem GmbH, Darmstadt, Germany), and lysed with a microfluidizer. Upon centrifugation, the filtered (0.45 µm) crude extract was loaded onto a 5 ml Ni^{2+}-HiTrap column (GE Healthcare, Munich, Germany) buffer $A^{NusG-CTD}$. The column was washed with 20 CVs buffer $A^{NusG-CTD}$ containing 10 mM imidazole and elution was carried out with a step gradient from 60 mM – 1 M imidazole in buffer $A^{NusG-CTD}$. Fractions containing the target protein were combined and dialyzed against buffer $A^{NusG-CTD}$ (MWCO 3.5 kDa) at 4 °C overnight in the presence of TEV protease to cleave off the tag. The dialysate was applied to three coupled 5ml Ni^{2+}-HiTrap columns (GE Healthcare, Munich, Germany) equilibrated with buffer $A^{NusG-CTD}$ to remove His_6-Gb1, uncut fusion protein, and TEV protease. The flow through was concentrated by

ultrafiltration (MWCO 3 kDa) and then subjected to a size exclusion chromatography using a HiLoad S75 column (GE Healthcare, Munich, Germany) equilibrated with buffer $B^{NusG-CTD}$ (25 mM HEPES (pH 7.5), 100 mM NaCl). Fractions containing pure NusG-CTD were combined and concentrated by ultrafiltration (MWCO 3 kDa), before being shock-frozen in liquid nitrogen and stored at -80 °C.

The production of the $S10^{\Delta}$:NusB heterodimer was done according to (Zuber et al., 2019). For expression, *E. coli* BL21 (λ DE3) cells (Novagen, Madison, WI, USA) containing plasmids pGEX-6P_*ecoNusE$^{\Delta}$* (encoding *E. coli* S10 where residues 46 - 67 were substituted by a single Ser ($S10^{\Delta}$) with an N-terminal glutathione S-transferase (GST)-tag followed by a PreScission protease cleavage site) or pET29b_*ecoNusB* (encoding tag-less *E. coli* NusB) were grown in ampicillin (100 μg/ml) or kanamycin (30 μg/ml) containing LB medium, respectively, at 37 °C to an OD_{600} of 0.5. The temperature was then lowered to 20 °C and over-expression was induced by addition of 0.5 mM IPTG after 30 min. Upon incubation overnight, cells were pelleted by centrifugation (6,000 x *g*). Cells containing $S10^{\Delta}$ or NusB, obtained from the same culture volume, were then resuspended in buffer $A^{S10_{\Delta}:NusB}$ (50 mM Tris/HCl (pH 7.5), 150 mM NaCl, 1 mM dithiothreitol (DTT)), supplemented with ½ protease inhibitor cocktail tablet (cOmplete, EDTA-free, Roche Diagnostics, Mannheim, Germany) and a small amount of DNase I (AppliChem GmbH, Darmstadt, Germany), mixed and subsequently lysed using a microfluidizer. The lysate was stirred for 30 min at 4 °C to allow formation of the $S10^{\Delta}$:NusB dimer. Cell debris was removed by centrifugation and the crude extract was applied to four coupled 5 ml GSTrap FF columns (GE Healthcare, Munich, Germany) equilibrated with buffer $A^{S10_{\Delta}:NusB}$. After washing with 20 column volumes (CVs) of buffer $A^{S10_{\Delta}:NusB}$ elution was performed in one step with buffer $A^{S10_{\Delta}:NusB}$ containing 15 mM reduced glutathione. PreScission protease was added to the combined target fractions and the protein solution was dialyzed against buffer $B^{S10_{\Delta}:NusB}$ (50 mM Tris/HCl (pH 7.5), 1 mM DTT)

overnight. The dialysate was subsequently applied to two 5 ml HiTrap Q XL columns coupled to two HiTrap SP XL columns (all from GE Healthcare. Munich, Germany) equilibrated with buffer $B^{S10_{\Delta}:NusB}$. The columns were washed with 20 CVs buffer $B^{S10_{\Delta}:NusB}$ and, after disconnecting, the $S10_{\Delta}$:NusB dimer was eluted from the two HiTrap SP XL columns with buffer $B^{S10_{\Delta}:NusB}$ containing 1 M NaCl. The protein solution was dialyzed against buffer $C^{S10_{\Delta}:NusB}$ (25 mM HEPES (pH 7.5), 100 mM NaCl), concentrated *via* ultrafiltration (MWCO 5 kDa), flash-frozen in liquid nitrogen, and stored at -80 °C.

RNAP was produced as described (Zuber et al., 2019). Expression was carried out in *E. coli* BL21 (λ DE3) cells (Novagen, Madison, WI, USA) harboring plasmid pVS10 (encoding *E. coli* core RNAP subunits α, β, β', and ω, with β carrying a C-terminal His_6-tag; (Svetlov and Artsimovitch, 2015)). Cells were grown at 37 °C in LB medium supplemented with ampicillin (100 μg/ml) to an OD_{600} of 0.7. The temperature was lowered to 16 °C and gene expression was induced by addition of 0.5 mM IPTG at OD_{600} = 0.8. Cells were harvested by centrifugation (6,000 x *g*, 10 min, 4 °C) after overnight incubation, resuspended in buffer A^{RNAP} (50 mM Tris/HCl (pH 6.9), 500 mM NaCl, 5 % (v/v) glycerol, 1 mM β-mercaptoethanol (β-ME)) containing 10 mM imidazole, DNase I (AppliChem GmbH, Darmstadt, Germany), and ½ protease inhibitor tablet (cOmplete, EDTA-free, Roche Diagnostics, Mannheim, Germany) and lysed with a microfluidizer. The lysate was centrifuged for 30 min at 13,000 rpm and 4 °C, and, subsequently, the supernatant was applied to a 40 ml Ni^{2+}-Chelating Sepharose column (GE Healthcare, Munich, Germany) equilibrated with buffer A^{RNAP} containing 10 mM imidazole. Upon washing with 25 CVs of buffer A^{RNAP} containing 10 mM imidazole RNAP was eluted using a gradient from 90 mM – 1 M imidazole in buffer A^{RNAP}. Fractions containing RNAP were combined, dialyzed against buffer B^{RNAP} (50 mM Tris/HCl (pH 6.9), 5 % (v/v) glycerol, 0.5 mM ethylenediaminetetraacetic acid (EDTA), 1 mM β-ME) containing 100 mM NaCl, and applied

to two 5 ml Heparin FF columns (GE Healthcare, Munich, Germany) equilibrated with buffer B^{RNAP} containing 100 mM NaCl. After washing with buffer B^{RNAP} containing 100 mM NaCl, the enzyme was eluted with a constant gradient from 100 mM to 1 M NaCl in buffer B^{RNAP}. RNAP-containing fractions were pooled, dialyzed against buffer C^{RNAP} (50 mM Tris/HCl (pH 6.9), 150 mM NaCl, 5 % (v/v) glycerol, 0.5 mM EDTA, 1 mM β-ME), and subsequently concentrated by ultrafiltration (MWCO 10 kDa) before being subjected to a SEC run using a HiLoad S200 column (GE Healthcare, Munich, Germany) equilibrated with buffer C^{RNAP}. Fractions containing pure core RNAP were concentrated by ultrafiltration (MWCO 10 kDa), glycerol was added to a final concentration of 50 % (v/v), and the solution was stored at -20 °C.

Intact 70S ribosomes were produced as follows. *E. coli* strain MRE600 cells grown in LB medium were harvested, lysed by passing through a French Press 3x at ~800 PSI, and clarified by a short centrifugation (20,000 rpm, 40 min) in opening buffer (20 mM Tris/HCl (pH 7.5), 100mM NH$_4$Cl, 10.5 mM Mg acetate, 0.5 mM EDTA, with half a protease inhibitor cocktail tablet (Roche, EDTA-free), and 1mM TCEP added just before use). The lysate was loaded onto the top of 5 mL sucrose cushion (20 mM Tris-HCl (pH 7.5), 500 mM NH$_4$Cl, 10.5 mM Mg acetate, 0.5 mM EDTA, 1.1 M sucrose, and 1 mM TCEP added before use) and centrifuged for 24 h at 28,000 rpm in a 70Ti rotor (Beckman Coulter, Inc.). The pellets were suspended in washing buffer (20 mM Tris-HCl (pH7.5), 500mM NH$_4$Cl, 10.5mM Mg acetate, 0.5 mM EDTA and 1 mM TCEP added before use), and centrifuged through a 10–35% (w/v) sucrose gradient for 19 h at 16,000 rpm in a SW28 rotor (Beckman Coulter, Inc.). Fractions containing the 70S ribosomes were pooled and kept at -80°C for further use. Ribosomes for NMR experiments were obtained from New England Biolabs.

Electron Microscopy. Purified 70S ribosomes were incubated with full-length NusG at a ratio of 1:7 for 40 min at room temperature, prior to blotting and plunge-freezing as

previously described (Grassucci et al., 2007). Data were collected on a TF30 Polara electron microscope (FEI, Portland, Oregon) at 300kV using a K2 Summit direct electron detector camera (Gatan, Pleasanton, CA). Images were recorded using the automated data collection system Leginon (Suloway et al., 2005) in counting mode, and taken at the nominal magnification of 32,000x, corresponding to a calibrated pixel size of 1.66Å.

Image processing. A total of 188,127 particles were automatically extracted from 1,327 images using Arachnid (Langlois et al., 2014). RELION (Scheres, 2012) 3D classification was used to resolve the heterogeneity of the particle images, and auto-refinement to further improve resolution for each class. The final refinement for the NusG-bound 70S class containing 17,122 particles yielded an average resolution of ~6.8Å (FSC=0.143; following "gold standard" protocol, see table S1).

Model refinement. The model refinement was performed in two stages; the first was molecular dynamics flexible fitting and the second was fine-tuning of the model using the real-space refinement function in Phenix.

In the first stage, the starting model was assembled from the X-ray structure of the *E. coli* 30S ribosomal subunit (PDB ID 4GD2) and the NMR solution structure of the NusG-CTD (PDB 2KVQ chain G). This starting model was first docked into the segmented maps of our 70S density map as a rigid body using UCSF Chimera (Pettersen et al., 2004). Then it was fitted into the segmented map using the Molecular Dynamic Flexibly Fitting (MDFF) method (Trabuco et al., 2008) and run using the NAMD program (Phillips et al., 2005) for 0.5 ns of simulation time, followed by 5,000 steps of energy minimization.

In the second stage, we performed rounds of real-space refinement using the program Phenix (Afonine et al., 2018) to correct geometry, rotamers and overlaps. Atomic positions from the model obtained by MDFF were also used as the reference model for restraints used

during the refinement to retain the secondary structure. To account for the relatively low resolution of the map, the parameters of *weight* and *nonbonded_weight* for the restraint terms were manually adjusted. The model was inspected, and problematic outliers were fixed using the program Coot (Emsley et al., 2010). The final model was validated using the program MolProbity (Williams et al., 2018).

NMR spectroscopy. NMR experiments were conducted on Bruker Ascend Aeon 900 and 1000 MHz spectrometers equipped with cryogenically cooled, inverse triple resonance probes at 298 K. NMR data was converted and processed using in-house software. 2D correlation spectra were visualized and analyzed with NMRViewJ (One Moon Scientific, Inc., Westfield, NJ, USA), 1D spectra were plotted using MatLab (The MathWorks, Inc., Version 9.2.0.538062). Resonance assignments for NusG methyl groups were taken from a previous study (Mooney et al., 2009).

[ILV]-NusG-CTD was in 10 mM K-phosphate (pH 7.5), 50 mM KCl, 1 mM $MgCl_2$, 99.9 % (v/v) D_2O, [ILV]-NusG-NTD in 50 mM Na-phosphate (pH 7.5), 50 mM KCl, 0.3 mM EDTA, 5 % (v/v) d_7-glycerol, 0.01 % (w/v) NaN_3, 99.9 % (v/v) D_2O. For the titration of [ILV]-NusG with RNAP and $S10^{\Delta}$:NusB, all proteins were in 50 mM Na-phosphate (pH 7.5), 50 mM KCl, 0.3 mM EDTA, 99.9 % (v/v) D_2O and 5 mM $MgCl_2$ and 2 mM DTT were added to the NMR sample to increase the-long-term stability of RNAP. For all interaction studies involving ribosomes and for the titration of [ILV]-NusG^{F165A} with $S10^{\Delta}$:NusB, all components were in 20 mM HEPES/KOH (pH 7.6), 10 mM Mg-acetate, 30 mM KCl, 7 mM β-ME, 10 % (v/v) D_2O. The titration of [ILV]-NusG^{F165A} with $S10^{\Delta}$:NusB was conducted in a 5 mm tube with an initial sample volume of 550 µl. All other measurements were carried out in 3 mm NMR tubes with an (initial) volume of 200 µl.

1D and 2D titration experiments were evaluated quantitatively by analyzing either changes in

signal intensity or changes in chemical shifts. If chemical shift changes were in the fast

regime on the chemical shift the normalized chemical shift perturbation ($\Delta\delta_{norm}$) was

calculated according to equation 1.

$$\Delta\delta_{norm} = \sqrt{\left(\Delta\delta\ ^1H\right)^2 + \left[0.25\left(\Delta\delta^{13}C\right)\right]^2} \qquad (1)$$

with $\Delta\delta$ being the resonance frequency difference between the initial and final state of the

titration (i.e. [ILV]-NusG:RNAP:S10$^\Delta$:NusB = 1:2:0:0 *vs.* 1:2:2:2) in ppm.

If the system was in slow or intermediate chemical exchange the signal intensities were

analyzed quantitatively. First, the intensity of each 1D spectrum or methyl group signal,

respectively, was normalized by the concentration of the [ILV]-labeled protein, the receiver

gain, the number of scans, and the length of the 90° ^1H pulse. Then the relative intensity, i.e.

the ratio of the normalized signal intensity of [ILV]-labeled protein in the respective titration

step to the normalized signal intensity of free [ILV]-labeled protein, was calculated and

plotted against the sequence of NusG or the NusG variant, respectively.

qRT-PCR. Total RNA was extracted from cells grown in M9 medium supplemented with

casamino acids (0.2%) at 37°C to mid-log phase (OD_{600}=0.3). Fold-increase of the PCR

product was determined using qRT-PCR. RNA was extracted from logarithmically growing

cultures (OD_{600}=0.2-0.3). Where indicated, cells were treated with BCM (100 mg/ml) 1 min

before induction with 1mM IPTG for *lacZ*. Samples were removed (0.5ml) at the indicated

times and total RNA extracted RNA extracted using Qiagen RNeasy and Qiagen RNAprotect

Bacteria Reagent (Qiagen, Germantown, MD). cDNA was synthesized from the samples

using High Capacity RNA to cDNA kit (ThermoFisher, Waltham, MA). qRT-PCR reactions

were performed using Taqman Gene Expression Master Mix (Thermofisher, Waltham, MA) and Biorad DNA Engine Opticon2 Real-Time Cycler (Bio-Rad Laboratories, Hercules, CA) and PrimeTime qPCR probes (Integrated DNA Technologies, Coralville, IA).

The *lacA* transcript was probed with the following probe:

5'-/56-FAM/CCACATGAC/ZEN/TTCCGATCCAGACGTT/3IABkFQ/-3';

primer 1:5'- ATACTACCCGCGCCAATAAC;

primer 2: 5'-CCCTGTACACCATGAATTGAGA).

The reference gene was *ompA*

(probe: 5'-/56-FAM/CAACAACAT/ZEN/CGGTGACGCACACAC /3IABkFQ/-3';

primer 1: 5'-TGACCGAAACGGTAGGAAAC;

primer 2: 5'-ACGCGATCACTCCTGAAATC).

The PCR was performed using the following conditions: 50 $^\circ$C for 10 min., 95 $^\circ$C for 2 min, followed by 40 cycles each of 95 °C for 15s, and 60 °C 1min; 50 nmol probe, 25 nmol primer 1, 25 nmol primer 2. Fold increases were calculated from measured C_t values using the $\Delta\Delta C_t$ method (Livak and Schmittgen, 2001). Read-through was calculated from the ratio of fold-increase of RNA level +/- BCM. Values are the average of three or more independent experiments and all reactions were performed in duplicate. The standard deviation of read-through was calculated using error propagation.

β-galactosidase assays. Cultures were grown in LB to early log phase (OD_{600} = 0.3) at 37 °C. Where indicated BCM (100 mg/ml) was added to inhibit Rho-dependent transcription termination prior to induction of *lacZ* with 1mm IPTG. Where indicated *λn* was expressed by incubation at 42 $^\circ$C. Reactions were terminated 15 min after induction. β-galactosidase was measured using a modification of the method of Miller (Zhang and Bremer, 1995). Read-

14

through was calculated from the ratio of β-galactosidase activity +/- BCM/λN. At least three replicates were performed per experiment and the resultant values were averaged. The standard deviation of read-through was calculated using error propagation.

Supplemental References

Afonine, P.V., Poon, B.K., Read, R.J., Sobolev, O.V., Terwilliger, T.C., Urzhumtsev, A., and Adams, P.D. (2018). Real-space refinement in PHENIX for cryo-EM and crystallography. Acta Crystallogr D Struct Biol *74*, 531-544.

Burmann, B.M., Scheckenhofer, U., Schweimer, K., and Rösch, P. (2011). Domain interactions of the transcription-translation coupling factor *Escherichia coli* NusG are intermolecular and transient. Biochem. J. *435*, 783–789.

Emsley, P., Lohkamp, B., Scott, W.G., and Cowtan, K. (2010). Features and development of Coot. Acta Crystallogr D Biol Crystallogr *66*, 486-501.

Grassucci, R.A., Taylor, D.J., and Frank, J. (2007). Preparation of macromolecular complexes for cryo-electron microscopy. Nat Protoc *2*, 3239–3246.

Langlois, R., Pallesen, J., Ash, J.T., Nam Ho, D., Rubinstein, J.L., and Frank, J. (2014). Automated particle picking for low-contrast macromolecules in cryo-electron microscopy. J. Struct. Biol. *186*, 1–7.

Livak, K.J., and Schmittgen, T.D. (2001). Analysis of relative gene expression data using real-time quantitative PCR and the 2(-Delta Delta C(T)) Method. Methods *25*, 402–408.

Meyer, O., and Schlegel, H.G. (1983). Biology of aerobic carbon monoxide-oxidizing bacteria. Annu. Rev. Microbiol. *37*, 277–310.

Mooney, R.A., Schweimer, K., Rösch, P., Gottesman, M., and Landick, R. (2009). Two structurally independent domains of *E. coli* NusG create regulatory plasticity *via* distinct interactions with RNA polymerase and regulators. J. Mol. Biol. *391*, 341–358.

Pettersen, E.F., Goddard, T.D., Huang, C.C., Couch, G.S., Greenblatt, D.M., Meng, E.C., and Ferrin, T.E. (2004). UCSF Chimera--a visualization system for exploratory research and analysis. J. Comput. Chem. *25*, 1605–1612.

Phillips, J.C., Braun, R., Wang, W., Gumbart, J., Tajkhorshid, E., Villa, E., Chipot, C., Skeel,

R.D., Kalé, L., and Schulten, K. (2005). Scalable molecular dynamics with NAMD. J. Comput. Chem. *26*, 1781–1802.

Sambrook, J., and Russel, D.W. (2001). Molecular Cloning: A Laboratory Manual (New York: Cold Spring Harbor Press).

Saxena, S., Myka, K.K., Washburn, R., Costantino, N., Court, D.L., and Gottesman, M.E. (2018). *Escherichia coli* transcription factor NusG binds to 70S ribosomes. Mol. Microbiol. *108*, 495–504.

Scheres, S.H.W. (2012). RELION: implementation of a Bayesian approach to cryo-EM structure determination. J. Struct. Biol. *180*, 519–530.

Sharan, S.K., Thomason, L.C., Kuznetsov, S.G., and Court, D.L. (2009). Recombineering: a homologous recombination-based method of genetic engineering. Nat. Protoc. *4*, 206–223.

Silhavy, T.J., Berman, M.L., and Enquist, L.W. (1984). Experiments with Gene Fusions (Cold Spring Harbor (NY): Cold Spring Harbor Laboratory Press).

Suloway, C., Pulokas, J., Fellmann, D., Cheng, A., Guerra, F., Quispe, J., Stagg, S., Potter, C.S., and Carragher, B. (2005). Automated molecular microscopy: the new Leginon system. J. Struct. Biol. *151*, 41–60.

Svetlov, V., and Artsimovitch, I. (2015). Purification of bacterial RNA polymerase: tools and protocols. Methods Mol. Biol. *1276*, 13–29.

Trabuco, L.G., Villa, E., Mitra, K., Frank, J., and Schulten, K. (2008). Flexible fitting of atomic structures into electron microscopy maps using molecular dynamics. Structure *16*, 673–683.

Williams, C.J., Headd, J.J., Moriarty, N.W., Prisant, M.G., Videau, L.L., Deis, L.N., Verma, V., Keedy, D.A., Hintze, B.J., Chen, V.B*., et al.* (2018). MolProbity: More and better reference data for improved all-atom structure validation. Protein Sci *27*, 293-315.

Zhang, X., and Bremer, H. (1995). Control of the *Escherichia coli rrnB* P1 promoter strength by ppGpp. J. Biol. Chem. *270*, 11181–11189.

Zuber, P.K., Schweimer, K., Rösch, P., Artsimovitch, I., and Knauer, S.H. (2019). Reversible fold-switching controls the functional cycle of the antitermination factor RfaH. Nat Commun *10*, 702.